Thermochimica Acta 608 (2015) 20–29

Contents lists available at ScienceDirect

Thermochimica Acta

journal homepage: www.elsevier.com/locate/tca

Curing kinetics of epoxy/alkyl phosphonium modified nanoclay composites for high performance applications

Marcela Elisabeth Penoff *, Matías Lanfranconi, Vera Alejandra Alvarez, Romina Ollier

Composite Materials Group (CoMP) – Material Science Institute (INTEMA), National Research Council (CONICET), Engineering Faculty – National University of Mar del Plata (UNMdP). Mar del Plata, Argentina. Juan B. Justo 4302, Mar del Plata 7600, Argentina

ARTICLE INFO

Article history:
Received 2 December 2014
Received in revised form 6 April 2015
Accepted 8 April 2015
Available online 9 April 2015

Keywords:
Nanocomposites
Clay
Kinetics
FTIR
MDSC
Thermosets

ABSTRACT

Alkyl phosphonium salts are novel and unexplored modifiers for polymer based composites which can improve the clays compatibility and dispersion in the polymer matrix. These salts can enhance the thermal stability of the modified clays, which is an indispensable requirement for thermosetting composites curing and processing occurring at high temperatures. In this work, a raw bentonite was ion exchanged with tributyl(hexadecyl) phosphonium bromide and then a novel epoxy/nanoclay composite was synthesized. The curing kinetics of the nanocomposites was studied. An extensively kinetic study was performed by FT-IR analysis and models accounting for many potential reactions and diffusion restrictions were proposed. A relationship between the H-bonding interactions and the kinetics was found. Also, the effect of the modifier of bentonite was found to affect the reaction yield.

1. Introduction

Epoxy-based thermosetting polymers are used in a variety of industrial applications, such us in adhesives, coatings, electronics and high performance composite materials, due to their excellent thermal, mechanical and chemical properties [1–3]. Epoxy resins reinforced with nanometer sized layered silicates have received great attention due to the possibility of improving several properties, like stiffness, strength, fire resistance, dimensional stability, shrinkage, among others, even at low filler loadings [4,5]. Untreated nanoclays, like bentonite, are not easily dispersed in most polymers because of their natural hydrophilicity, and thus they are incompatible with organic polymers [6]. For this reason, clays can be chemically modified through ion exchange reactions with organic cations to enhance the interfacial interactions and promote the intercalation of polymers into the interlayer galleries, therefore, facilitating the formation of an exfoliated structure [7].

Many authors have reported the improvement of various properties of epoxy/clay nanocomposites by incorporating alkyl ammonium modified organoclays [8,9]. It has also been studied that loading of the alkyl ammonium exchanged montmorillonite in the epoxy matrix facilitates the curing reaction of epoxy based nanocomposites [10–12]. However, the incorporation of ammonium modified clays into thermoset matrices is limited because of their poor thermal stability. The same problem has been found for melt compounding and injection molding of thermoplastic polymer nanocomposites at high processing temperatures exceeding 200 °C [13,14]. In contrast, alkyl phosphonium salts enhance the thermal stability of the organoclays [15,16], which is necessary for the curing and processing of the composite materials with high performance applications, for example in windmill blades, petroleum pipelines and automotive pieces. There are few reports on the systematic study of epoxy resins loaded with alkyl phosphonium exchanged organoclays to improve the thermal and mechanical properties [17,18]. Nevertheless, there are no reports regarding the effect of alkyl phosphonium modified clays on the curing reaction or kinetic of epoxy resins.

The first challenge to overcome when preparing an epoxy/nanoclay composite is to disperse (intercalate or exfoliate) the nanoclays. XDR is a suitable and commonly used technique to verify the clay dispersion. The second challenge is to keep the matrix chemical and structural properties, such as curing and crosslinking degrees, to a level which does not negatively affect the mechanical properties, chemical stability and other features intended to get improved with the modification.

Normally, the structure and properties of epoxy/clay nanocomposites depend on the formation of the crosslinked molecular network, which is frequently influenced by the curing mechanism and kinetics of curing of the epoxy resin that involves several chemical reactions [19]. The knowledge of the cure process in the

* Corresponding author. Tel.: +54 223 481 6600.
E-mail address: elisabeth@fi.mdp.edu.ar (M.E. Penoff).

http://dx.doi.org/10.1016/j.tca.2015.04.008
0040-6031/

epoxy system is crucial to get a better control of the cure reactions and, as result, to optimize the properties of the final product [20]. One of the most widely used techniques for studying the kinetics of the cure reaction of epoxy systems is the thermal analysis by differential scanning calorimetry (DSC), in isothermal or dynamic modes [21]. Modulated differential scanning calorimetry (MDSC) is a newer technique which allows getting more information about a thermal process. In conventional DSC, an isothermal or linear time/temperature program is used. After subtraction of the empty pan curve, correction for heat transport effects and calibration, one gets the curve of the heat flow rate $Q(t)$ into the sample versus temperature. In modulated-temperature DSC, the common temperature program is superimposed with a dynamic temperature change (sinusoidal in most cases). The measured signal is influenced by heat transfer conditions which change both the amplitude and the phase shift. After subtraction of the empty pan measurement under the same conditions and calibration, the heat flow rate into the sample $Q(t)$ can be calculated from the measured signal. The measured heat flow rate is usually separated into the underlying heat flow rate Q_u (this is approximately the conventional DSC curve) and the dynamic component Q_d. One method employed for the determination of these curves, which is commercially used by MDSC (TA-Instruments), is the procedure published by Reading and co-workers [22–25]. In this method, the reversing component of the heat flow rate, Q_{rev}, is calculated from the dynamic component; whereas, the so-called non-reversing component $Q_{non\text{-}rev}$ is the difference between Q_u and Q_{rev} [26]. In order to measure the heat of reaction, free from the sensible heat, the non-reversing heat flow is used [27].

Another powerful technique widely used to follow kinetic processes, is the Fourier transform infrared spectroscopy (FTIR). In particular, near infrared spectroscopy (NIR) provides a quantitative technique where glass sample holders can be used, with the advantage of a practical experimental setup to monitor a rather thick reactive sample. Besides, OH signals can be well detected, quantified, and a reasonable differentiation of their chemical associations can be attained [28–29]. Conversion – time curves from FTIR experiments can be used to compare the evolution of reaction with time, and thus to confirm the observations made by MDSC.

A better understanding of the experimental MDSC and FTIR data could be achieved by proposing a kinetic mechanistic model which describes all the reactions taking place in the system. Although the epoxy – amine system has been widely studied, the physical processes which take place during the polymerization complicate the interpretation of the experimental data. Vitrification is a phenomenon which slows the reaction rate due to a loss in the reactive groups' mobility. In an isothermal cure process, vitrification will be always observed if the curing temperature (T_c) is selected in the range between the unreacted systems glass transition temperature (Tg_0) and the glass transition temperature of the fully cured network (Tg_∞). This isothermal trajectory leads to a lower final conversion than the unity ($x<1$), limited by vitrification. A post curing step at $T>Tg_\infty$ is needed to attain the complete conversion ($x=1$). An isothermal curing trajectory at $T_c>Tg_\infty$ leads to complete conversion, but due to high values of reaction heat and polymerization rate, it is usually not possible to keep isothermal conditions. The sample temperature continuously increases as it is impossible to dissipate the reaction heat at the rate at which it is generated [30]. Kinetic mechanistic models have been proposed for curing temperatures above Tg_∞. These approaches consider that the general reactions which can take place during epoxy – amine polymerization are: epoxy – primary amine, epoxy – secondary amine, etherification and homopolymerization. Etherification only occurs at high temperatures [30,31] and homopolymerization requires the presence of a Lewis base or acid [32]. Epoxy – amine reactions can proceed catalyzed by OH groups. OH may be initially present in the reactive mixture and they are always formed by the reaction between epoxy and amino groups. Epoxy monomers contain OH in their chains, which can catalyze the polymerization from the beginning of the process, and in the systems here studied, where nanoclays are incorporated to the reactive system, OH are present in the clays platelets. These OH, also initially present in the reactive mixture, may or may not play a role in the curing kinetics. Besides, and despite drying the reactants and clays, traces of water retained in the hydrophilic bentonite may also contribute OH catalytic groups [33,34]. Also the formation of an epoxy – hydroxyl complex was proposed in the literature, which can be in equilibrium [34] or out of equilibrium [35].

In the case of the isothermal curing trajectories below Tg_∞, not only a chemical limiting factor restricts the conversion, but also a diffusional limiting term must be considered. Accordingly, the overall kinetic rate constant k is expressed in terms of a reaction-limited term (k_{chem}) and a diffusion-limited one (k_{diff}) [36,37]:

$$\frac{1}{k}=\frac{1}{k_{chem}}+\frac{1}{k_{diff}} \quad (1)$$

Chern and Poehlein [38] proposed a very simple equation coming from the free volume theory to estimate the ratio of the diffusion-controlled to reaction limited rate constant:

$$\frac{k_{diff}}{k_{chem}}=\exp[-C(x-x_c)] \quad (2)$$

where C is a constant which depends on the structure, system and curing temperature and x_c is a critical conversion. For values of conversion significantly lower than x_c, diffusion control is negligible. This allows determining the chemical kinetic constant for conversions lower than x_c and then employing this value when fitting the whole conversion curve, adjusting only the diffusional parameters [39].

The critical conversion responds to the conversion from which vitrification becomes efficient. The value of x_c has been reported to be similar to the gel conversion at low temperatures, and higher as temperature increases, approaching Tg_∞ [39].

There are no many reports which consider models for both regimes, below and above Tg_∞. In general, researchers select one of the two regimes to make the kinetic analysis [39–42].

In this work, epoxy/organo-modified nanoclay composites were prepared. Pristine and tributyl(hexadecyl) phosphonium exchanged bentonites were used to obtain the composites. The influence of both, bentonite and organo-bentonite, in the epoxy – amine reactions, was studied by means of MDSC and FTIR. A kinetic model was proposed and used together with FTIR data with the aim of understanding the changes occurred in the reaction parameters.

2. Experimental

2.1. Materials

A commercial diglycidyl ether of bisphenol A resin, DGEBA (DER 383, Dow chemicals) having epoxy equivalent about 176–183 g eq^{-1} and a viscosity of 9000–10,500 mPa.s at 25 °C, and triethylenetetramine (TETA, Novarchem S.A.), the hardener, were employed. The clay in the study was a bentonite supplied by Minarmco S.A. (Argentina). The cation exchange capacity (CEC) of bentonite was found to be 0.939 meq g^{-1}, measured by the methylene blue method [43]. The organic modifier used to exchange the pristine bentonite was tributyl(hexadecyl) phosphonium bromide provided by Sigma Aldrich, EEUU.

2.2. Sample preparation

Modification of bentonite with tributyl(hexadecyl) phosphonium bromide [43,44]: 2.5 g of clay were dispersed in 100 ml of deionized water. Then, the aqueous solution of tributyl(hexadecyl) phosphonium bromide of the corresponding concentration was added (0.9 times the CEC of the bentonite). The mixture was stirred for 2 h at 70 °C. After that, the suspension was filtered through a Buchner Funnel and washed with deionized water until free of bromide. The organoclay was dried with a spray dry system.

Epoxy/clay mixtures: The DGEBA monomer was mixed with neat and modified bentonites in order to study the influence of the pre-reaction procedure on the final material.

Epoxy/clay nanocomposites: The epoxy resin matrix and nanocomposites were prepared using a stoichiometric ratio between epoxy resin and hardener. The clays were previously dried at 100 °C for 2 h. The mixture of resin and nanoclay was prepared in the appropriate quantities in order to obtain materials with the desired content of clay (3 wt.%) and mixed by hand for 1 min. The mixture was then placed in an ultrasound bath for 5 min at room temperature. Due to the excellent epoxy – amine solubility, the amine was added and the system was homogenized by hand.

2.3. Characterization

2.3.1. X-ray diffraction (XRD)

XRD patterns of neat and modified bentonites, DGEBA/clays mixtures and nanocomposites were obtained from a PANanalytical X'Pert PRO diffractometer (Holland) equipped with a monochromatic CuKα radiation source (λ = 1.5406 Å) operating at 40 kV, 40 mA, at a scanning rate of 2° per min and a step size of 0.02°.

2.3.2. Modulated DSC

MDSC experiments were conducted in TA-Q2000 (TA Instruments, USA) calorimeter with a temperature amplitude variation of ±1 °C with a period of 60 s, under nitrogen flow. About 10 mg of the reactive mixture before curing was placed in an aluminum pan, and the sample was tested immediately after sealing and positioning it right on the sample cell. Each sample was tested twice and a fresh sample was prepared before every experimental determination.

First, each mixture was isothermically cured at 60 or 150 °C, this stage will be referred as the "Iso stage". Then, the sample was cooled to 25 °C. A modulated dynamic scan was performed at 3 °C min^{-1} until 200 °C, this stage was denoted "Ramp 1". These samples were then cooled to 25 °C. Finally, they were reheated to 200 °C at 10 °C min^{-1}, concluding the stage named "Ramp 2". The Iso step allowed curing up to a certain degree which would result in a rubbery or vitrified system. Only the total heat flow was registered in this step. The total heat flow of Ramp 1 can be split into the reversing and non-reversing heat flow. From the last signal, the residual heat of reaction of an incomplete cured system could be obtained. Besides, the *Tg* of the partially cured system ($Tg_{x<1}$) would be detected in the reversing heat flow [45]. As Ramp 1 reaches 200 °C, the system would completely cure, allowing Ramp 2 to register the *Tg* of the completely cured network (Tg_{∞}) or at least, the *Tg* of the thermoset with the maximum degree of curing achieved in this procedure.

2.3.3. FTIR

FTIR analyses were performed using Nicolet 6700 spectrometer (Thermo Scientific, USA). The spectra were recorded from 4000 to 7500 cm^{-1} (NIR range) with a resolution of 4 cm^{-1} and 32 scans. In the NIR range, the most important functional groups involved in the curing process, such as epoxy, primary and secondary amine, and hydroxyl functional groups, can be correctly isolated from the neighboring absorptions [46]. Small amounts of the reactive mixtures were deposited between two circular 3 mm thick glasses separated by an *o*-ring. Once they were in the oven, their FTIR spectra were recorded, at the selected temperature (60 or 150 °C), every 1 min until the treatment had completely finished (at least 120 min). The initial point at time = 0 was recorded at room temperature to avoid the advance of the reaction during the heating.

The cure process was studied by evaluating the decrease of the specific band of the epoxide functional group. For each sample, the progress in the curing reaction was followed by calculating the curing conversion:

$$x = 1 - \frac{A(t)}{A(0)} \tag{3}$$

where $A(t)$ and $A(0)$ are the reduced absorbances at time t and at starting time, respectively, corresponding to the epoxy combination band at 4530 cm^{-1} [33]. The band of the benzene group which appears at 4620 cm^{-1} was chosen as an invariant reference band and was used to calculate the reduced absorbance for epoxide functional groups [47]. Additionally, the primary amine concentration was followed by monitoring the peak at 4930 cm^{-1}, corresponding to the $-NH_2$ bending-stretching combination [48]. Although the kinetic model was fitted with the epoxy conversion, it was compared with the primary amine conversion curve to confirm the best fitting had been achieved. The OH attached to the polymer chains can be found at 4790 cm^{-1} and OH vibrations corresponding to water are responsible for the band at 5240 cm^{-1} [49].

2.4. Kinetic modeling

Fourth order Runge Kutta numerical method was used to solve the set of differential equations and the kinetic parameters were found using the least squares method to minimize the difference between the experimental and calculated conversion values.

2.4.1. Model 1

Let the brackets indicate concentration, A_1 a primary amino hydrogen, A_2 the secondary amino hydrogen generated by the reaction of a primary one, A_{2i} are the initially present secondary amino hydrogen, E the epoxy groups, OH the hydroxyl groups formed during the reaction and OH_i the hydroxyl groups initially present in the system (OH present in the DGEBA monomer and OH from the nanoclays, in the composites) and consider the system of Eqs. (4)–(9).

$$\frac{d[A_1]}{dt} = -2k_1[A_1][E][OH] - 2k_2[A_1][E][OH_i] \tag{4}$$

$$\frac{d[E]}{dt} = -k_1([A_1][E][OH] + [E][A_2][OH]) - k_2([A_1][E][OH_i] + [E][A_{2i}][OH_i]) - k_3[E][A_{2i}][OH] \tag{5}$$

$$\frac{d[OH]}{dt} = k_1([A_1][E][OH] + [E][A_2][OH]) + k_2[A_1][E][OH_i] + k_3[E][A_{2i}][OH] \tag{6}$$

$$\frac{d[A_2]}{dt} = k_1([A_1][E][OH] - [E][A_2][OH]) + k_2[A_1][E][OH_i] \tag{7}$$

$$\frac{d[A_3]}{dt} = k_1[E][A_2][OH] + k_2[E][A_{2i}][OH_i] + k_3[E][A_{2i}][OH] \quad (8)$$

$$\frac{d[A_{2i}]}{dt} = -k_2[E][A_{2i}][OH_i] - k_3[E][A_{2i}][OH] \quad (9)$$

Then, the reactions described are: (1) epoxy – primary amino groups reaction, catalyzed by the newly formed OH groups, with a rate constant k_1, (2) epoxy – secondary amino group when the amino hydrogen was generated by the reaction of a primary amino hydrogen, catalyzed by newly formed OH groups, characterized by a rate constant k_1, (3) epoxy – primary amino groups catalyzed by initially present OH groups, characterized by k_2 rate constant, and (4) epoxy – secondary amino groups when the amino hydrogen was initially present in the curing agent, catalyzed by initially present OH groups, with a rate constant k_2, (5) epoxy – secondary amino groups when the amino hydrogen was initially present in the curing agent, catalyzed by newly formed OH groups, given by a k_3 rate constant.

It has already been found in the literature [34,39,50], and proved in this work while searching for the best fitting model, that the reaction rate of the primary and secondary amino groups with epoxy is the same, thus well described by a unique kinetic parameter k_1. It has also been previously considered a kinetic model accounting for the uncatalyzed reactions, but this consideration was found to be useless for the best data fitting.

In the systems here studied there are different hydroxyl groups, those present in the clay platelets and those present in the resin and formed during the reaction, the two last being chemically similar and different from those of the nanoclays. It was found that independently if the OH groups that catalyze the epoxy – amine reaction are the formed or the initially present, the ratio of the primary/secondary amine reactivity remains unaltered.

2.4.2. Model 2

An epoxy – hydroxyl complex was reported to be in equilibrium [34] (see Eq. (10)) or out of equilibrium [35].

$$E + OH \Leftrightarrow EOH \quad (10)$$

Here, EOH (a complex formed with hydroxyls formed in the reaction) and EOH_i (a complex formed with initially present hydroxyls) were proposed to be out of equilibrium. EOH_i was introduced in accordance to the existence of OH_i and because EOH alone did not prove to fit the data.

The set of proposed reactions was:

$$E + OH \rightarrow EOH(k_e) \quad (11)$$

$$EOH \rightarrow E + OH(k'_e) \quad (12)$$

$$E + OH_i \rightarrow EOH_i(k_{ei}) \quad (13)$$

$$EOH_i \rightarrow E + OH_i(k'_e) \quad (14)$$

$$A_1 + EOH \rightarrow A_2 + 2OH(k_1) \quad (15)$$

$$A_1 + EOH_i \rightarrow A_2 + OH + OH_i(k_1) \quad (16)$$

$$A_2 + EOH \rightarrow A_3 + 2OH(k_1) \quad (17)$$

$$A_2 + EOH_i \rightarrow A_3 + OH + OH_i(k_1) \quad (18)$$

The reaction rate constants of Eqs. (11)–(18) may be all different. The similitude arose from the data fitting. So the rate equations become:

$$\frac{d[A_1]}{dt} = -2k_1([A_1][EOH] + [A_1][EOH_i]) \quad (19)$$

$$\frac{d[E]}{dt} = -k_e[E][OH] - k_{ei}[E][OH_i] + k'_e([EOH] + [EOH_i]) \quad (20)$$

$$\frac{d[OH]}{dt} = -k_e[E][OH] + k'_e[EOH] + k_1(2[A_1][EOH] + 2[A_2][EOH] + [A_1][EOH_i] + [A_2][EOH_i]) \quad (21)$$

$$\frac{d[A_2]}{dt} = k_1([A_1][EOH_i] - [A_2][EOH] - [A_2][EOH_i]) \quad (22)$$

$$\frac{d[EOH]}{dt} = k_e[E][OH] - k'_e[EOH] - k_1([A_1][EOH] + [A_2][EOH]) \quad (23)$$

$$\frac{d[EOH_i]}{dt} = k_{ei}[E][OH_i] - k'_e[EOH_i] - k_1([A_1][EOH_i] + [A_2][EOH_i]) \quad (24)$$

$$\frac{d[OH_i]}{dt} = -k_{ei}[E][OH_i] + k_1([A_1][EOH_i] + [A_2][EOH_i]) \quad (25)$$

3. Results and discussion

The samples used to study the curing reaction are the neat epoxy resin, MATRIX, i.e., a stoichiometric mixture of DGEBA and TETA; the resin modified with 3 wt.% of neat bentonite, BENT, and the resin modified with 3 wt.% of tributyl(hexadecyl) phosphonium bromide exchanged bentonite, TBHP.

3.1. XDR characterization

Fig. 1 shows the XRD patterns of the clay powders and the finally cured epoxy/clay nanocomposites. The basal spacing (d_{001}) was calculated from Bragg's law:

$$d = \frac{\lambda}{2\sin(\theta)} \quad (26)$$

The d-spacing of the clays were found to be 1.2 and 2.2 nm for the neat bentonite and for the exchanged one, respectively (Fig. 1a). The increase in the interlayer spacing of the organobentonite was due to the presence of alkylphosphonium ions inside the gallery regions.

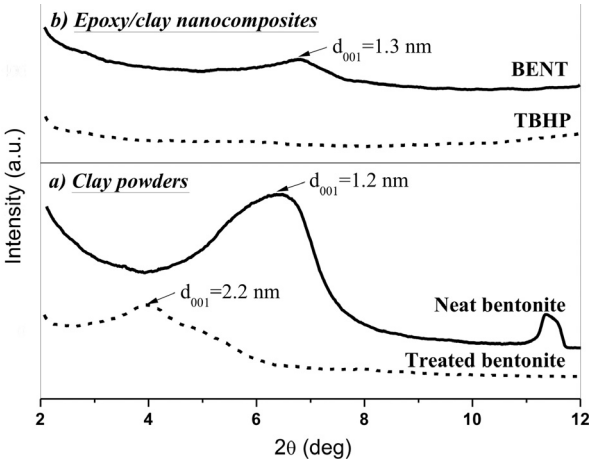

Fig. 1. XRD patterns of: (a) clay powders; (b) epoxy/clay nanocomposites.

The position of the diffraction peak of the clay in the BENT sample (Fig. 1b) did not shift towards lower angles indicating that exfoliation of the platelets did not occur and, thus, a lack of compatibility between the matrix and the untreated bentonite. On the other hand, XRD pattern of the cured epoxy filled with the organoclay, TBHP sample, did not show any diffraction peak corresponding to the d_{001} interlayer spacing of the organoclay. This can be attributed to the loss of orientation, and thus exfoliation, of the clay platelets within the epoxy matrix. Hence, the organoclay is well dispersed in the composite and it is a suitable filler with a great potential to improve the matrix properties. At the light of these results, the first challenge to be overcame when preparing a composite, i.e., the dispersion of the filler, can be perfectly accomplished by modifying the bentonite with tributyl(hexadecyl) phosphonium bromide before incorporating it to the epoxy matrix.

3.2. MDSC characterization

The MDSC cycles were chosen on the basis of the vitrification phenomenon described by Williams and Pascault [30]. An isothermal curing below Tg_∞ at 60 °C and another one above Tg_∞ at 150 °C were selected. The thermal results are summarized in Table 1. The first isothermal trajectory led to $x < 1$ and vitrification was observed. A residual heat of reaction after the isothermal curing confirmed that vitrification was responsible for the reaction limit. The second isothermal trajectory, at 150 °C, allowed registering the *Tg* of the material at the highest degree of curing, but the heat of reaction data was missed because the system cured rapidly and the reaction proceeded during the heating ramp up to the temperature set point.

The curves of the isothermal curing at 60 °C (see Fig. 2) shows a faster reaction rate for the BENT and TBHP samples compared to MATRIX. In spite of this difference, $Tg_{x<1}$ were all similar with a

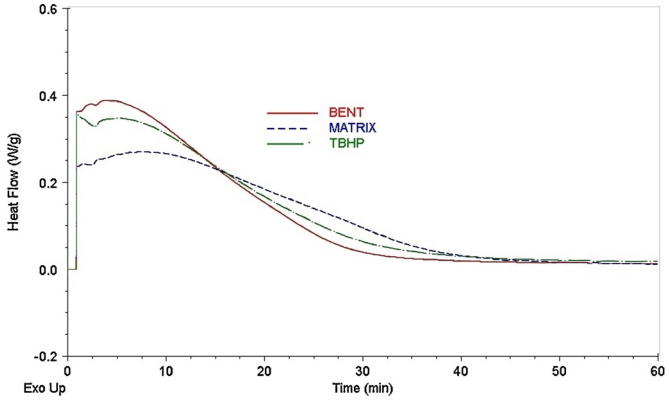

Fig. 2. Isothermal heat flow curves at 60 °C.

value of 77 °C. This is in agreement with the literature [30] which predicts, in general, a *Tg* of the incomplete reacted network 20–30 °C above the curing temperature. These results would imply that no structural differences occurred during the polymerization.

It can be observed in Fig. 2 that MATRIX reacted slower than the composites during the isothermal step, thus presented a higher residual heat of reaction (Fig. 3,Table 1). BENT showed the fastest reaction in both stages, the isothermal and dynamic ones. The faster reaction could be a consequence of a catalytic effect caused by OH groups present in the nanoclay and absent in the MATRIX [51]. These hydroxyls may belong to the silanol groups which are present in the surface of the clay platelets. The TBHP sample shows an intermediate case, with a slight increase in the reaction rate with respect to the MATRIX. This behavior can be attributed to the fact that the hydrophilicity of the organoclay is lower, so there are less trapped water molecules, and also to the fact that the

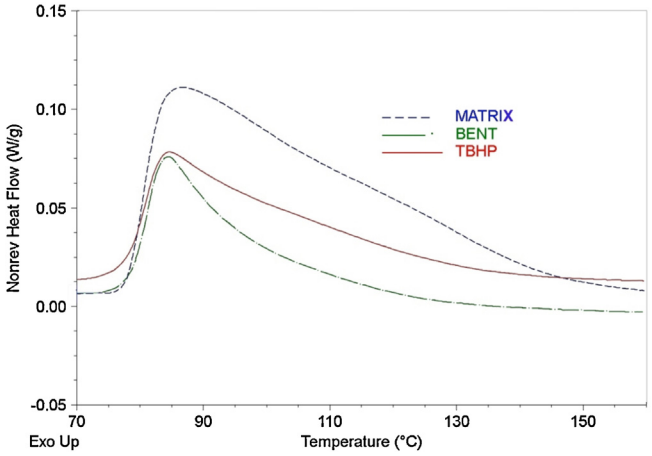

Fig. 3. Non-reversing heat flow during heating at 3 °C/min, modulated ± 1 °C every 60 s, after the isothermal treatment at 60 °C.

Table 1
MDSC results for matrix and nanocomposites.

Temperature of isothermal curing (°C)	Property	Sample		
		MATRIX	BENT	TBHP
60	ΔH_{iso} (kJ eq^{-1})	73.1	87.5	91.1
	Tg (°C)	77.0 ± 0.3	77.2 ± 0.7	77.1 ± 0.4
	Residual ΔH_{din} (kJ eq^{-1})	17.5	5.5	7.8
	ΔH_{tot} (kJ eq^{-1})	90.6	93.0	98.9
	Tg_∞ (°C)	142.0 ± 0.6	142.7 ± 0.8	145.0 ± 0.9
150	Tg_∞ (°C)	143.0 ± 0.7	145.0 ± 0.9	137.0 ± 0.6

organoclay has an organic content of almost 30 wt.%, so the concentration of OH groups is lower compared to BENT sample.

TBHP was the only sample which almost reached the theoretical total heat of reaction of 105 ± 5 kJ/eq$_{epoxy}$ [33,52–55]. The lower total heats of reaction of MATRIX and BENT could imply an incomplete conversion in these samples, in accordance to their slightly lower *Tg* after the dynamic curing stage. However, it would not be accurate to calculate the degrees of conversion from these thermal data, since it is very probable that part of the heat of the isothermal reaction had been missed from registry during the sample preparation and heating ramp up to the temperature set point.

Data shown in Table 1 demonstrate that the highest *Tg* registered was 145 °C, in accordance to previous experiments of the work team. This is expected to be the glass transition temperature of the fully cured network, i.e., Tg_∞. The isothermal curing at 150 °C led to a BENT network with Tg_∞ = 145 °C, a MATRIX network with Tg_∞ = 143 °C, i.e., thermosets of complete and almost complete conversion, but a TBHP network with a Tg_∞ = 137 °C which clearly has not reached a complete conversion. Due to the mentioned errors carried out in MDSC experiments (missing heat of reaction data) conversion values will be discussed on the basis of FTIR results, and will be useful to look for a kinetic model.

3.3. FTIR and kinetic mechanistic modeling

FTIR measurements are expected to be more accurate than MDSC to determine the epoxy – amine kinetics because the initial points at time = 0 can be collected at room temperature avoiding the advance of reaction during the heating ramp. Of course some error would prevail at the higher temperatures, but would only affect the initial times of reaction, i.e., the lower conversion values.

The reactions of epoxy – amine systems can be summarized as shown in Fig. 4 [30]. As it was mentioned in the introduction section, etherification occurs only at high temperatures and homopolymerization needs the presence of a Lewis base or acid [30,31]. 150 °C is not expected to be a high enough temperature to allow the etherification, but an experimental confirmation is needed. Concerning homopolymerization, OH groups that are present in the nanoclays could play the role of the Lewis base, so this reaction should also be experimentally discarded.

First, DGEBA – bentonite and DGEBA – organobentonite mixtures were prepared without the hardener and analyzed by FTIR at 150 °C. No epoxy consumption was observed at the highest temperature employed for the kinetic study, so etherification can be neglected at all the temperatures used, and the OH of the clays showed no participation in the hompolymerization reaction.

With the aim of understanding the influence of OH groups of the nanoclays on the epoxy – amine curing kinetics, the Model 1 was proposed taking into account the main factors affecting the curing process. The conversion – time curves were obtained from FTIR experiments for MATRIX, BENT and TBHP samples. The selected temperatures for the kinetic study were 60, 120 and 150 °C, including a vitrification process at 60 °C, a curing temperature above Tg_∞ (150 °C) and an intermediate case at 120 °C, in accordance to MDSC studies.

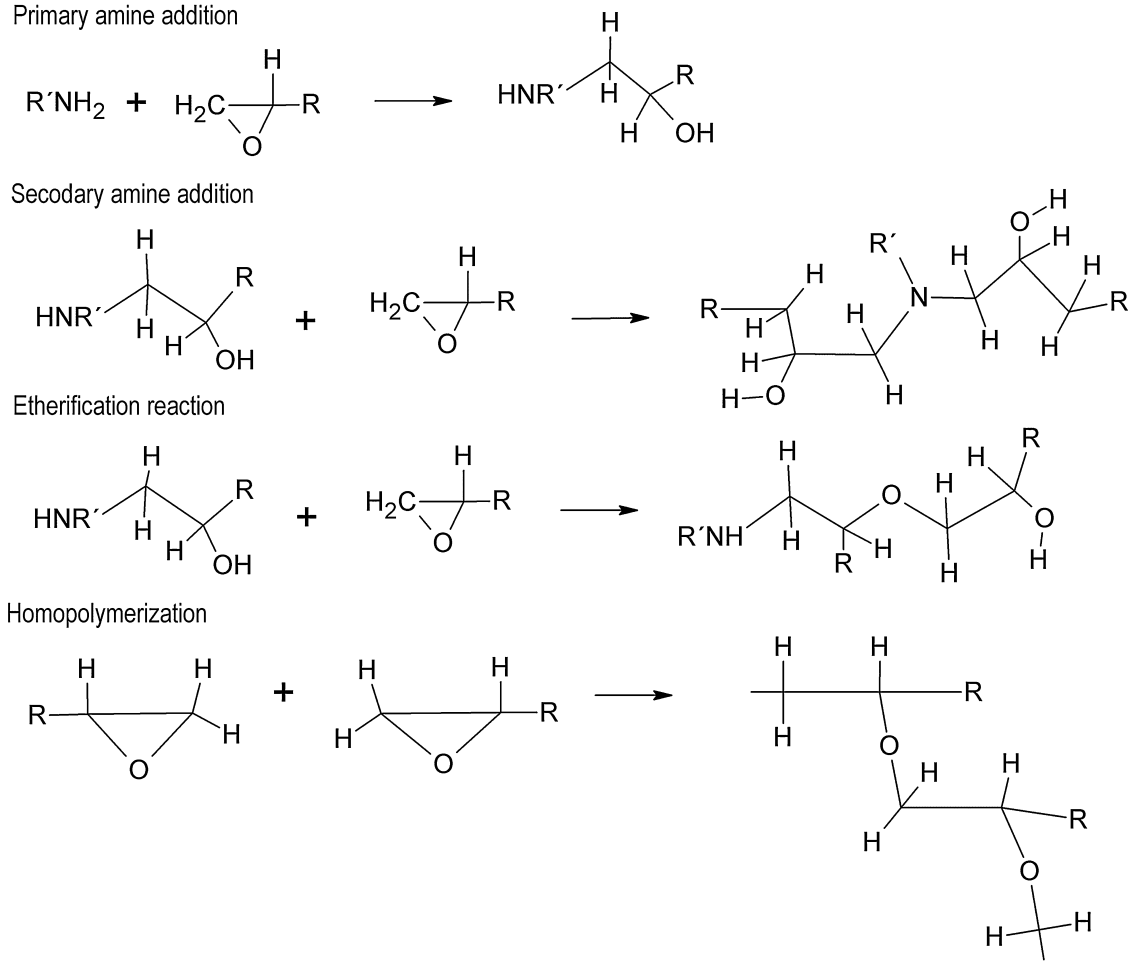

Fig. 4. Possible reactions taking place in the epoxy – amine mixtures.

In this model some missing values could not be included, these are the initial hydroxyl concentration [OH_i] when nanoclays are present in the reactive formulation, because the OH content in the nanoclays is not known neither easy to be determined. Besides, the value needed for the modeling is the effective amount of OH in the surface of the clays, capable to participate in the reaction mechanism. Also, traces of water may contribute some hydroxyls in each sample, which may affect the [OH_i] as well. In all the cases, the known initial hydroxyl concentration coming from DGEBA monomer was used in the model, which might introduce some error. This error would be specially reflected in the k_2 results, so this rate constant will be considered separately.

The values of the kinetic parameters used to model the curing kinetics are listed in Table 2. k_3 values are very similar to those of k_1; in general k_3 is lower than k_1 at low temperatures and becomes higher at elevated temperatures. For TBHP samples, differences were negligible. The diffusional limiting parameters x_c and C, needed to fit the data at 60 °C are also listed. Figs. 5–7 compare the experimental and the modeled epoxy conversion curves. The images of these figures are separated for better visibility clarity.

The model for the conversion curves at 60 °C fits very well the experimental data. C values resulted independent of temperature, a tendency already reported in the literature [39]. The x_c value was higher for TBHP sample, which suggests that in that system chains may have a better mobility while reaching the final conversion at that temperature.

Reaction rates are very similar, but slightly increase in the order MATRIX < TBHP < BENT. The shape of the conversion curves is very similar at 60 °C, indicative of similar reaction mechanisms. These findings are in accordance with MDSC results.

At higher temperatures, differences in the conversion curves arise, as it can be seen in Fig. 6. While BENT conversion starts increasing from initial times, MATRIX is delayed. TBHP is an intermediate case and it is analyzed separately in Fig. 7, since more differences are encountered. At 150 °C TBHP does not achieve the complete conversion, as it was mentioned when analyzing the MDSC data. When considering the better fitting for 60, 80 (not shown) and 120 °C, Arrhenius law predicts an overestimated conversion curve at 150 °C than the experimentally found. This may be indicative of a change in the mechanism of the reaction. It has been reported than the clay modifiers can alter the conversion yield. Huskić et al. [56] found a marked decrease of the conversion yield in poly(methyl-metacrylate) (PMMA) polymer when mixed with montmorillonite (MMT) modified with cetyl-trimethylammonium bromide (CTMAB). They demonstrated that the CTMAB was the responsible for the final conversion reduction, not the MMT.

Continuing with the general analysis, when looking at the data at the three temperatures for all the formulations, a more pronounced delay exists at higher temperatures. Although the model fitting seems deficient at initial times (0–3 min) for MATRIX (see Fig. 6), it represents the process quite well. As it was discussed, initial conversions would carry the error of the reaction advance during the heating up to the set point, so it is not strange having difficulties to fit the initial values at 150 °C.

An analysis of the influence of each kinetic parameter in the conversion – time curves, showed that the delay in the reaction starting is achieved with lower k_2 values. Table 3 shows the k_2 values for the three formulations at each temperature.

Except for a few values, k_2 decreases with temperature generally, in contradiction with the Arrhenius law. This failure in the model allowed identifying the process which is in disagreement. As it was mentioned previously, k_2 values would carry an error from the unknown [OH_i] data for composites. But in the case of the MATRIX this is a theoretically calculated value.

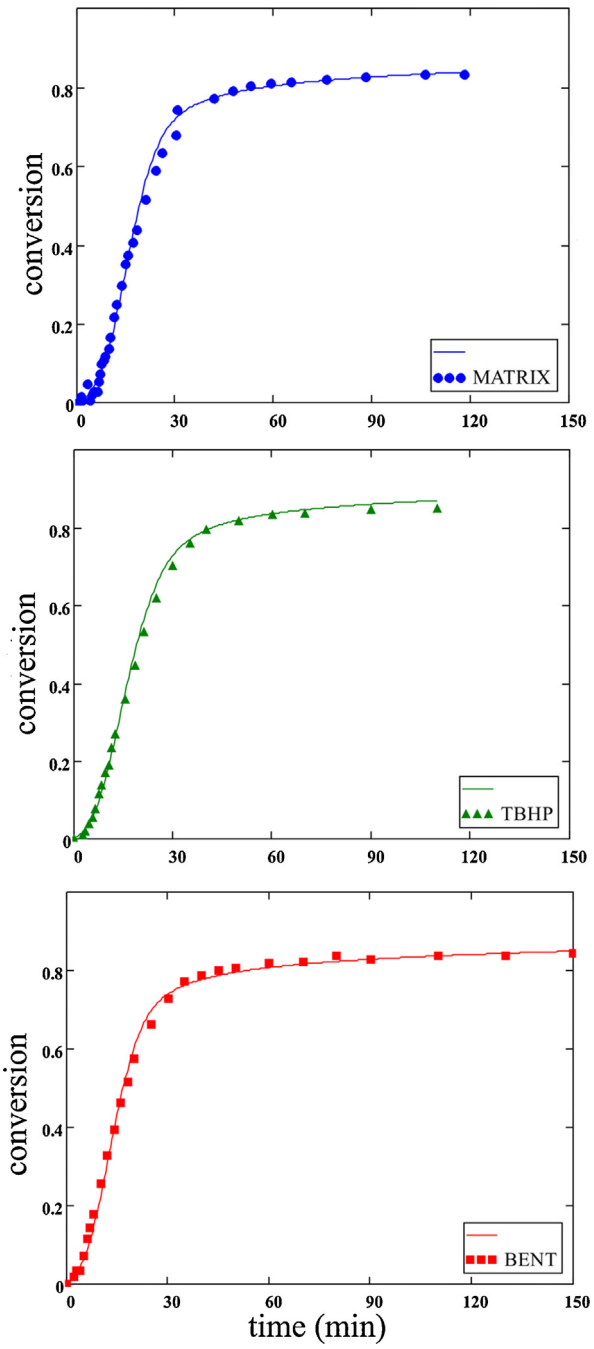

Fig. 5. Experimental (symbols) and model (lines) conversion curves at 60 °C.

Table 2
Kinetic parameters studied in the range 60–150 °C.

Parameter	Sample		
	MATRIX	BENT	TBHP
A_{k1} ($kg^2\,eq^{-2}\,s^{-1}$)	$1.310 \cdot 10^3$	$5.398 \cdot 10^3$	$1.900 \cdot 10^3$
E_A ($kJ\,mol^{-1}$)	43.3 ± 2.7	47.3 ± 3.1	44.9 ± 1.9
A_{k3} ($kg^2\,eq^{-2}\,s^{-1}$)	$4.691 \cdot 10^3$	$1.232 \cdot 10^4$	$1.900 \cdot 10^3$
E_A ($kJ\,mol^{-1}$)	47.7 ± 2.8	50.1 ± 3.3	44.9 ± 2.1
x_c (60 °C)	0.726	0.726	0.783
C^a (60 °C)	5	5	5

[a] The C values tabulated are those used in the system of equations of the reaction rates expressed in concentration, not conversion as in Eq. (2).

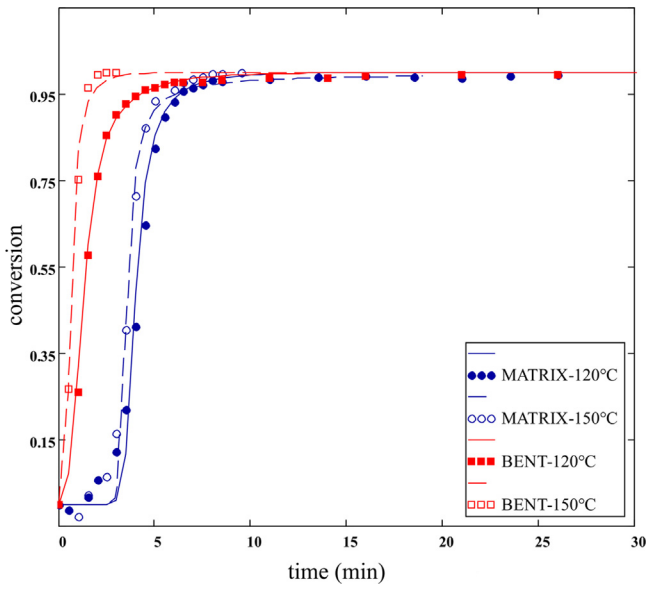

Fig. 6. BENT and MATRIX experimental (symbols) and model (lines) conversion curves at 120 and 150 °C.

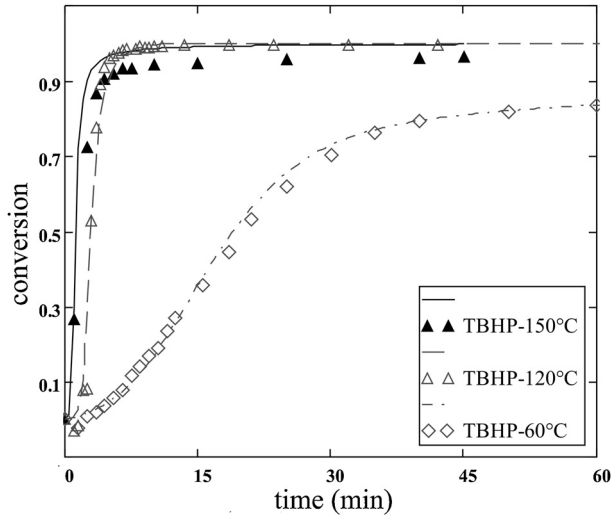

Fig. 7. TBHP experimental (symbols) and model (lines) conversion curves.

Moreover, MATRIX has the most pronounced deviation from Arrhenius law. It is reported in the literature [34,35] that the concentration of an epoxy – hydroxyl complex can decrease with temperature in the epoxy – amine reaction systems. The existence of such a complex with the mentioned dependence on temperature could be in agreement with the Model 1 failure. With the aim of finding out if a model accounting for a complex could fit the data, the Model 2 was used to compare the conversion curves of the MATRIX, at those temperatures where no diffusion restrictions take place. Here the purpose is only to find out the behavior of the kinetic constants with temperature, no activation energy is calculated, thus, fitting the data with two temperatures is enough.

The formation of the EOH_i, i.e., the ke_i, depends inversely on temperature, contrary to the predictable result, although EOH showed the expected dependence. Table 4 exemplifies the kinetic parameters employed to fit the MATRIX data with the Model 2. This model failure can be discussed on the bases of FTIR spectra's interesting features at initial times.

The OH peak at 4790 cm^{-1} increases with time as OH groups are formed by the epoxy – amine reaction, as expected. Simultaneously, the peak at 5240 cm^{-1}, which is assigned to the OH vibrational transition of absorbed water [57], was found, indicating that at least traces of water may be present in the reactive mixtures. Water hydroxyls are susceptible to catalyze the epoxy reactions [47]. The results of Choi's study suggested that even a small amount of water which is absorbed during the course of curing or during storage condition could significantly accelerate the rate of cure reactions for epoxies. This would explain why MATRIX sample needed the introduction of OH_i in the kinetic model in order to fit the conversion data: water hydroxyls are chemically different from those belonging to the DGEBA monomer, so it is necessary to differentiate those hydroxyls. Moreover, if water molecules were present, then the calculated $[OH_i]$ value, regarding the DGEBA monomer's hydroxyls, would not be accurate. The unknown $[OH_i]$, which additionally should not be necessarily the same at different temperatures, would explain the kinetic model failure. Lower rate constants found at higher temperatures would be a consequence of lower $[OH_i]$, actually. Bearing in mind that $[OH_i]$ comes in part from water, it is reasonable to think that water can be lost by evaporation at higher temperatures. Besides, it would not be possible to find all the missing parameters in the set of reaction rate equations of the kinetic model, with the actual experimental data: reaction rate constants could be found if the amount $[OH_i]$ were known, but determining also the $[OH_i]$ from the same set of data would make the method unreliable. However, the aim of this work is to elucidate the influence of the chemical species in the reaction media. Bearing this in mind, the solution to the rate equations and the parameters found will be used in order to correlate the following experimental facts.

It was already explained that the near infrared (NIR) peak at 5240 cm^{-1} corresponds to water absorbance. However, the evolution of the peak's intensity over time would be intriguing if considering it only represents water concentration.

Fig. 8 shows the relative peak intensity at 5240 cm^{-1} calculated as:

$$\frac{A_t/A_{ref,t}}{A_0/A_{ref,0}} \quad (27)$$

where A_t is the absorbance at any time, A_0 is the absorbance at initial time and A_{ref} is the absorbance of the reference species at 4620 cm^{-1}.

Table 3
Kinetic constants for the reactions catalyzed by initially present OH groups, k_2, at different curing temperatures.

Sample	k_2 value ($kg^2\,eq^{-2}\,s^{-1}$)		
	60 °C	120 °C	150 °C
MATRIX	$5.83\cdot10^{-5}$	$3.00\cdot10^{-8}$	$1.58\cdot10^{-14}$
BENT	$1.03\cdot10^{-4}$	$7.83\cdot10^{-4}$	$3.00\cdot10^{-4}$
TBHP	$8.00\cdot10^{-5}$	$1.52\cdot10^{-5}$	$2.83\cdot10^{-5}$

Table 4
Kinetic parameters for the model accounting for epoxy – hydroxyl complexes.

Parameter	Temperature	
	120 °C	150 °C
k_1 ($kg\,eq^{-1}\,s^{-1}$)	8.5×10^{-3}	1.5×10^{-2}
k_e ($kg\,eq^{-1}\,s^{-1}$)	1.35×10^{-2}	1.42×10^{-2}
k'_e (s^{-1})	1.35×10^{-6}	1.13×10^{-5}
k_{ei} (s^{-1})	6.83×10^{-4}	2.83×10^{-4}

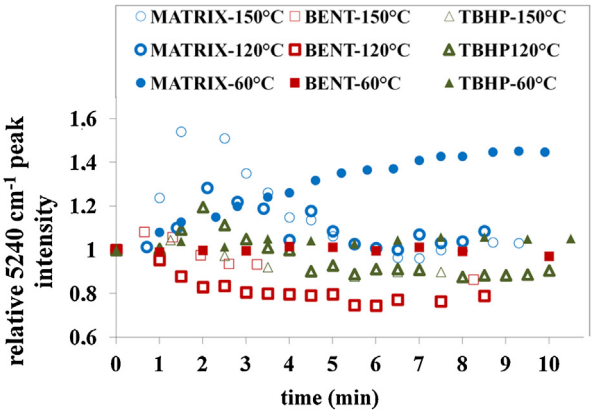

Fig. 8. 5240 cm^{-1} NIR relative peak intensity evolution with time for all the samples at the three studied temperatures.

It is evident that in the MATRIX sample, the intensity increases during the first few minutes, and then falls to its initial value. At 60 °C there is an increment and very low diminution and in the case of composites, only for TBHP at 120 °C the maximum exists, the rest of the samples show only the intensity decrease. In order to account for the observed changes in the NIR spectra of the OH species, it can be remarked that: (i) no apparent cause exists to enhance the absorbed water in the reactive mixture, neither water is formed in any reaction in the studied system, (ii) an enhancement of the absorbance in the NIR spectrum can be caused by the intensity of the physical interactions between the chemical groups. Musto et al. have already reported such an increase in an OH signal in the NIR and they attributed it to the enhancement of the absolute integrated intensity, i.e., a physical factor rather than a chemical one [28]. Looking at the 6690 cm^{-1} signal, associated with the O—H overtones, together with the 5240 cm^{-1} one, for DGEBA and DGEBA – modified bentonite mixture, heated at 150 °C, the following relative peak intensity changes occur: 6690 cm^{-1} intensity increases while 5240 cm^{-1} decreases. For these samples the epoxy signal at 4530 cm^{-1} remained unaltered, as mentioned when discarding etherification and homopolymerization reactions. These facts support the idea of OH signals changes being due to H-bondings rearrangements. Apparently, the 5240 cm^{-1} peak enhancement is related to the reaction rate retardation.

Bearing in mind the comments made about the usage of the kinetic model with qualitative purposes, the [EOH_i] predicted evolution with time can be compared to the experimental NIR changes, in order to make a correlation. The model predicts a [EOH_i] enhancement at initial times, going through a maximum at around 2 min (see Fig. 9). In coincidence, at these short times, the NIR signal at 5240 cm^{-1} markedly changes. This fact supports the idea of the reaction rate being highly affected by the H-bondings interactions at short times: a reactive intermediate which is strongly affected by H-bondings participate in the reaction path and its concentration is expected to be maximum (i.e., its influence in the reaction rate is expected to be stronger) when those force – interaction changes take place.

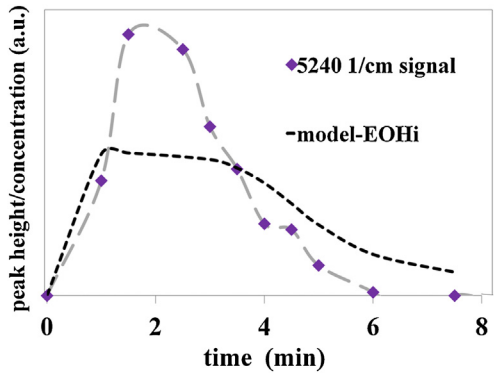

Fig. 9. Time evolution of the 5240 cm^{-1} relative peak intensity and modeled EOH_i concentration, for MATRIX at 150 °C.

All the experimental evidence, together with the mismatch in the proposed kinetic models, indicates that the initial hydroxyls in the reactive mixtures account for the kinetic changes observed in the samples studied. Regarding the composites, it is then possible that a higher initial [OH_i] coming from some water content in the hydrophilic nanoclays accelerates the reaction compared to MATRIX, but hydroxyls inherent to the nanoclays platelets may cause the same effect. It is also possible that the presence of the nanoclays changes the hydroxyl interactions among the species present in the reactive mixture, generating the reaction rate enhancement.

Although there are many reports about water addition influence in the curing kinetics of epoxy based systems [47,58–59] there is no information about the effect of traces of water retained in high temperature reactive mixtures even after the reactants drying procedure, which may not be a hundred percent effective. Even after drying, a small amount of water is susceptible to be retained within the liquid monomers structure. When curing at high temperatures (above 100 °C) these retained water molecules could be released in some extent. Moreover, if hydrophilic clays are incorporated to the reactive system, the water retention by the reactants can be severely affected and change the curing kinetics of the neat matrix.

4. Conclusions

FTIR was an adequate technique to perform the curing kinetic study of epoxy resin/nanoclays based composites. No homopolymerization neither etherification reactions were found to occur in composites or polymer matrix formulations.

For the first time, tributyl(hexadecyl) phosphonium bromide was used to modify bentonite nanoclays employed in composites and its influence in their curing kinetics was analyzed. This modifier was found to be responsible for the reduction of the reaction yield of the epoxy – amine system.

Several models representing the curing kinetics of the resin matrix and composites were proposed and extensively analyzed. Together with FTIR data, these models helped to identify the factor which caused the changes in the kinetic curves between composites and MATRIX. It was found that traces of water initially present in the system accelerate the reaction rate, even when the reactants were previously dried. Curing at high temperatures apparently modifies the initial water concentration. Composites present higher reaction rates, originated in a faster reaction onset, which can be attributed to a higher concentration of water molecules coming from the nanoclays, to the presence of hydroxyls in the nanoclays laminae or to different H-bonding interactions among the reactive species at initial times.

At the light of the results found, it is for the first time stated that the incorporation of alkyl phosphonium modified bentonite can improve the thermal stability needed in composites processing with no apparent detriment of the curing process.

Acknowledgements

The authors would like to acknowledge Dr. J. Morán for his collaboration and the financial support of the National Research Council of Argentina (CONICET), National University of Mar del

Plata (UNMdP) and the National Agency of Scientific and Technologic Promotion (ANPCyT), Fonarsec FSNano004.

References

[1] K. Mitra, Assessing optimal growth of desired species in epoxy polymerization under uncertainty, Chem. Eng. J. 162 (2010) 322–330.
[2] T.-H. Liou, Kinetics study of thermal decomposition of electronic packaging material, Chem. Eng. J. 98 (2004) 39–51.
[3] J. Abenojar, M.A. Martínez, M. Pantoja, F. Velasco, J.C. Del Real, Epoxy composite reinforced with nano and micro SiC particles: curing kinetics and mechanical properties, J. Adhes. 88 (2012) 418–434.
[4] J.M. Brown, D. Curliss, R.A. Vaia, Thermoset-layered silicate nanocomposites. quaternary ammonium montmorillonite with primary diamine cured epoxies, Chem. Mater. 12 (2000) 3376–3384.
[5] T. Lan, T.J. Pinnavaia, Clay-reinforced epoxy nanocomposites, Chem. Mater. 6 (1994) 2216–2219.
[6] S. Pavlidou, C.D. Papaspyrides, A review on polymer–layered silicate nanocomposites, Prog. Polym. Sci. 33 (2008) 1119–1198.
[7] T.D. Ngo, M.T. Ton-That, S. Hoa, K. Cole, Curing kinetics and mechanical properties of epoxy nanocomposites based on different organoclays, Polym. Eng. Sci. 47 (2007) 649–661.
[8] P.I. Xidas, K.S. Triantafyllidis, Effect of the type of alkylammonium ion clay modifier on the structure and thermal/mechanical properties of glassy and rubbery epoxy–clay nanocomposites, Eur. Polym. J. 46 (2010) 404–417.
[9] X. Kornmann, H. Lindberg, L.A. Berglund, Synthesis of epoxy–clay nanocomposites: influence of the nature of the clay on structure, Polymer 42 (2001) 1303–1310.
[10] M.T. Ton-That, T.D. Ngo, P. Ding, G. Fang, K. Cole, S. Hoa, Epoxy nanocomposites: analysis and kinetics of cure, Polym. Eng. Sci. 44 (2004) 1132–1141.
[11] S. Montserrat, F. Román, J. Hutchinson, L. Campos, Analysis of the cure of epoxy based layered silicate nanocomposites: reaction kinetics and nanostructure development, J. Appl. Polym. Sci. 108 (2008) 923–938.
[12] M. Ivankovic, I. Brnardic, H. Ivankovic, H.J. Mencer, DSC study of the cure kinetics during nanocomposite formation: epoxy/poly(oxypropylene) diamine/organically modified montmorillonite system, J. Appl. Polym. Sci. 99 (2006) 550–557.
[13] W. Abdallah, U. Yilmazer, Polyamide 66 nanocomposites based on organoclays treated with thermally stable phosphonium salts, J. Appl. Polym. Sci. 127 (2013) 772–783.
[14] W. Abdallah, U. Yilmazer, Preparation and characterization of thermally stable phosphonium organoclays and their use in poly(ethylene terephthalate) nanocomposites, J. Appl. Polym. Sci. 128 (2013) 4283–4293.
[15] V. Mittal, Modification of montmorillonites with thermally stable phosphonium cations and comparison with alkylammonium montmorillonites, Appl. Clay Sci. 56 (2012) 103–109.
[16] J.U. Calderon, B. Lennox, M.R. Kamal, Thermally stable phosphonium-montmorillonite organoclays, Appl. Clay Sci. 40 (2008) 90–98.
[17] K. Saitoh, K. Ohashi, T. Oyama, A. Takahashi, J. Kadota, H. Hirano, K. Hasegawa, Development of high-performance epoxy/clay nanocomposites by incorporating novel phosphonium modified montmorillonite, J. Appl. Polym. Sci. 122 (2011) 666–675.
[18] M.S. Lakshmi, B. Narmadha, B.S.R. Reddy, Enhanced thermal stability and structural characteristics of different MMT-Clay/epoxy-nanocomposite materials, Polym. Degrad. Stab. 93 (2008) 201–213.
[19] L. Li, H. Zou, M. Liang, Y. Chen, Study on the effect of poly(oxypropylene) diamine modified organic montmorillonite on curing kinetics of epoxy nanocomposties, Thermochim. Acta 597 (2014) 93–100.
[20] V.S. Souza, O. Bianchi, M.F.S. Lima, R.S. Mauler, Morphological, thermomechanical and thermal behavior of epoxy/MMT nanocomposites, J. Non-Cryst. Solids 400 (2014) 58–66.
[21] X. Xiong, R. Ren, S. Liu, S. Lu, P. Chen, The curing kinetics and thermal properties of epoxy resins cured by aromatic diamine with hetero-cyclic side chain structure, Thermochim. Acta 595 (2014) 22–27.
[22] P. Gill, S. Sauerbrunn, M. Reading, Modulated differential scanning calorimetry, J. Therm. Anal. Calorim. 40 (1993) 931–939.
[23] M. Reading, A. Luget, R. Wilson, Modulated differential scanning calorimetry, Thermochim. Acta 238 (1994) 295–307.
[24] M. Reading, Modulated differential scanning calorimetry—a new way forward in materials characterization, Trends Polym. Sci. 1 (1993) 248–253.
[25] M. Reading, D. Elliott, V. Hill, A new approach to the calorimetric investigation of physical and chemical transitions, J. Therm. Anal. Calorim. 40 (1993) 949–955.
[26] J.E.K. Schawe, A comparison of different evaluation methods in modulated temperature DSC, Thermochim. Acta 260 (1995) 1–16.
[27] S. Montserrat, J.G. Martı'n, Non-isothermal curing of a diepoxide–cycloaliphatic diamine system by temperature modulated differential scanning calorimetry, Thermochim. Acta 388 (2002) 343–354.
[28] P. Musto, M. Abbate, G. Ragosta, G. Scarinzi, A study by Raman near-infrared and dynamic-mechanical spectroscopies on the curing behaviour, molecular structure and viscoelastic properties of epoxy/anhydride networks, Polymer 48 (2007) 3703–3716.
[29] H.W. Siesler, Y. Ozaki, S. Kawata, H.M. Heise, Near-Infrared Spectroscopy: Principles, Instruments, Applications, John Wiley & Sons, 2008.
[30] J.P. Pascault, H. Sautereau, J. Verdu, R.J.J. Williams, Thermosetting Polymers, Taylor & Francis, New York, 2002.
[31] A.A. Azeez, K.Y. Rhee, S.J. Park, D. Hui, Epoxy clay nanocomposites–processing, properties and applications: a review, Compos. Part B 45 (2013) 308–320.
[32] J.V. Crivello, J.H.W. Lam, Diaryliodonium salts. a new class of photoinitiators for cationic polymerization, Macromolecules 10 (1977) 1307–1315.
[33] M.E. Penoff, G. Papagni, M.J. Yañez, P.E. Montemartini, P.A. Oyanguren, Synthesis and characterization of an epoxy based thermoset containing a fluorinated thermoplastic, J. Polym. Sci. Part B: Polym. Phys. 45 (2007) 2781–2792.
[34] C.C. Riccardi, F. Fraga, J. Dupuy, R.J.J. Williams, Cure kinetics of diglycidylether of bisphenol A–ethylenediamine revisited using a mechanistic model, J. Appl. Polym. Sci. 82 (2001) 2319–2325.
[35] M. Blanco, M.A. Corcuera, C.C. Riccardi, I. Mondragon, Mechanistic kinetic model of an epoxy resin cured with a mixture of amines of different functionalities, Polymer 46 (2005) 7989–8000.
[36] C.W. Wise, W.D. Cook, A.A. Goodwin, Chemico-diffusion kinetics of model epoxy-amine resins, Polymer 38 (1997) 3251–3261.
[37] K. Cole, J. Hechler, D. Noel, A new approach to modeling the cure kinetics of epoxy/amine thermosetting resins. 2. Application to a typical system based on bis [4-(diglycidylamino) phenyl] methane and bis (4-aminophenyl) sulfone, Macromolecules 24 (1991) 3098–3110.
[38] C.S. Chern, G.W. Poehlein, A kinetic model for curing reactions of epoxides with amines, Polym. Eng. Sci. 27 (1987) 788–795.
[39] E.G. Karayannidou, D.S. Achilias, I.D. Sideridou, Cure kinetics of epoxy–amine resins used in the restoration of works of art from glass or ceramic, Eur. Polym. J. 42 (2006) 3311–3323.
[40] C.C. Su, E.M. Woo, Y.P. Huang, Curing kinetics and reaction-induced homogeneity in networks of poly(4-vinyl phenol) and diglycidylether epoxide cured with amine, Polym. Eng. Sci. 45 (2005) 1–10.
[41] J. Macan, I. Brnardić, M. Ivanković, H.J. Mencer, DSC study of cure kinetics of DGEBA-based epoxy resin with poly(oxypropylene) diamine, J. Therm. Anal. Calorim. 81 (2005) 369–373.
[42] S. Montserrat, J.G. Martín, The isothermal curing of a diepoxide-cycloaliphatic diamine resin by temperature modulated differential scanning calorimetry, J. Appl. Polym. Sci. 85 (2002) 1263–1276.
[43] D.A. D'Amico, R.P. Ollier, V.A. Alvarez, W.F. Schroeder, V.P. Cyras, Modification of bentonite by combination of reactions of acid-activation, silylation and ionic exchange, Appl. Clay Sci. 99 (2014) 254–260.
[44] R. Ollier, A. Vazquez, V. Alvarez, Biodegradable nanocomposites based on modified bentonite and polycaprolactone, in: Z. Bartul, J. Trenor (Eds.), Advances in Nanotechnology, Nova Publishers, New York, 2011, pp. 281–301.
[45] C. Tomasi, P. Mustarelli, N.A. Hawkins, V. Hill, Characterisation of amorphous materials by modulated differential scanning calorimetry, Thermochim. Acta 278 (1996) 9–18.
[46] G. Li, Z. Huang, P. Li, C. Xin, X. Jia, B. Wang, Y. He, S. Ryu, X. Yang, Curing kinetics and mechanisms of polysulfone nanofibrous membranes toughened epoxy/amine systems using isothermal DSC and NIR, Thermochim. Acta 497 (2010) 27–34.
[47] S. Choi, A.P. Janisse, C. Liu, E.P. Douglas, Effect of water addition on the cure kinetics of an epoxy-amine thermoset, J. Polym. Sci. Part A: Polym. Chem. 49 (2011) 4650–4659.
[48] F.J. Johnson, W.M. Cross, D.A. Boyles, J.J. Kellar, Complete system monitoring of polymer matrix composites, Compos. Part A 31 (2000) 959–968.
[49] Q. Wang, B.K. Storm, L.P. Houmøller, Study of the isothermal curing of an epoxy prepreg by near-infrared spectroscopy, J. Appl. Polym. Sci. 87 (2003) 2295–2305.
[50] H.J. Flammersheim, Kinetics and mechanism of the epoxide–amine polyaddition, Thermochim. Acta 310 (1998) 153–159.
[51] K.S. Seo, D.S. Kim, Curing behavior and structure of an epoxy/clay nanocomposite system, Polym. Eng. Sci. 46 (2006) 1318–1325.
[52] B.A. Rozenberg, Kinetics, thermodynamics and mechanism of reactions of epoxy oligomers with amines, in: K. Dušek (Ed.), Epoxy Resins and Composites II, Springer Berlin Heidelberg, 1986, pp. 113–165.
[53] K. Horie, H. Hiura, M. Sawada, I. Mita, H. Kambe, Calorimetric investigation of polymerization reactions. III. Curing reaction of epoxides with amines, J. Polym. Sci. A-1 Polym. Chem. 8 (1970) 1357–1372.
[54] S. Swier, G. Van Assche, B. Van Mele, Reaction kinetics modeling and thermal properties of epoxy–amines as measured by modulated-temperature DSC. I. Linear step-growth polymerization of DGEBA + aniline, J. Appl. Polym. Sci. 91 (2004) 2798–2813.
[55] J.M. Barton, The Application of Differential Scanning Calorimetry (DSC) to the Study of Epoxy Resin Curing Reactions, Epoxy Resins and Composites I, Springer, 1985, pp. 111–154.
[56] M. Huskić, E. Žagar, M. Žigon, The influence of a quaternary ammonium salt and MMT on the in situ intercalative polymerization of PMMA, Eur. Polym. J. 48 (2012) 1555–1560.
[57] G. Lachenal, Y. Ozaki, Advantages of near infrared spectroscopy for the analysis of polymers and composites, Macromol. Symp. 141 (1999) 283–292.
[58] L. Wu, S.V. Hoa, M.T. Ton-That, Effects of water on the curing and properties of epoxy adhesive used for bonding FRP composite sheet to concrete, J. Appl. Polym. Sci. 92 (2004) 2261–2268.
[59] J. Chen, T. Nakamura, K. Aoki, Y. Aoki, T. Utsunomiya, Curing of epoxy resin contaminated with water, J. Appl. Polym. Sci. 79 (2001) 214–220.